

Radiosensitizer-eluting nanocoatings on gold fiducials for biological *in-situ* image-guided radio therapy (BIS-IGRT)

This article has been downloaded from IOPscience. Please scroll down to see the full text article.

2010 Phys. Med. Biol. 55 6039

(<http://iopscience.iop.org/0031-9155/55/20/001>)

View [the table of contents for this issue](#), or go to the [journal homepage](#) for more

Download details:

IP Address: 129.10.128.214

The article was downloaded on 23/05/2011 at 19:32

Please note that [terms and conditions apply](#).

Radiosensitizer-eluting nanocoatings on gold fiducials for biological *in-situ* image-guided radio therapy (BIS-IGRT)

D K Nagesha^{1,3}, D B Tada^{1,3}, C K K Stambaugh¹, E Gultepe¹, E Jost¹,
C O Levy¹, R Cormack², G M Makrigiorgos² and S Sridhar^{1,2,4}

¹ Electronic Materials Research Institute and Department of Physics, Northeastern University, Boston, MA 02115, USA

² Department of Radiation Oncology, Dana Farber Cancer Institute, Brigham and Women's Hospital, Harvard Medical School, Boston, MA, USA

E-mail: s.sridhar@neu.edu

Received 7 April 2010, in final form 27 August 2010

Published 21 September 2010

Online at stacks.iop.org/PMB/55/6039

Abstract

Image-guided radiation treatments (IGRT) routinely utilize radio-opaque implantable devices, such as fiducials or brachytherapy spacers, for improved spatial accuracy. The therapeutic efficiency of IGRT can be further enhanced by biological *in situ* dose painting (BIS-IGRT) of radiosensitizers through localized delivery within the tumor using gold fiducial markers that have been coated with nanoporous polymer matrices loaded with nanoparticles (NPs). In this work, two approaches were studied: (i) a free drug release system consisting of Doxorubicin (Dox), a hydrophilic drug, loaded into a non-degradable polymer poly(methyl methacrylate) (PMMA) coating and (ii) poly(D,L-lactic-co-glycolic acid) (PLGA) NPs loaded with fluorescent Coumarin-6, serving as a model for a hydrophobic drug, in a biodegradable chitosan matrix. Temporal release kinetics measurements in buffer were carried out using fluorescence spectroscopy. In the first case of free Dox release, an initial release within the first few hours was followed by a sustained release over the course of the next 3 months. In the second platform, release of NPs and the free drug was controlled by the degradation rate of the chitosan matrix and PLGA. The results show that dosage and rate of release of these radiosensitizers coated on gold fiducials for IGRT can be precisely tailored to achieve the desired release profile for radiation therapy of cancer.

(Some figures in this article are in colour only in the electronic version)

³ These authors contributed equally to this work.

⁴ Author to whom any correspondence should be addressed.

1. Introduction

The radiation dose delivered to tumors by external beam radiation therapy (XRT) is limited by the dose that is also unavoidably delivered to nearby normal tissue. Image-guided radiation therapy (IGRT) uses daily pre-treatment imaging to localize the target and reduce the volume of normal tissue being irradiated. X-ray imaging is widely available in the XRT treatment room, but is not well suited to distinguish soft tissues such as tumor and normal tissues. To assist in localizing the tumor, radio-opaque markers may be placed in the target using minimally invasive techniques (Xie *et al* 2008, Friedland *et al* 2009, Wurm *et al* 2006). Pretreatment imaging can easily localize the markers, or fiducials, and use them as a surrogate for the position of the target. The fiducials are essential to localize the tumor and target the radiation, but presently provide no direct therapeutic benefit.

Acting as radiosensitizers, drugs can increase the effectiveness of radiation. Two examples of radiosensitizers are Doxorubicin (Dox) (molecular weight 579.98 g mol⁻¹) and Taxotere (m.w. 861.93 g mol⁻¹) that generally also have cytotoxic effects on their own and are often used as chemotherapeutic agents (Doiron *et al* 1999, Kumar 2003). As a result, normal tissue toxicities limit the doses of these drugs that can be delivered systemically. Timed release of *in situ* applied radiosensitizers has also been attempted (Garcia-Garcia *et al* 2006, Li *et al* 2004) in order to achieve localized delivery of chemotherapeutic agents.

Modifying IGRT fiducials to provide *in vivo* localized delivery of radiosensitizer to a tumor in addition to guiding beam delivery offers an opportunity to improve the therapeutic ratio of radiation therapy without introducing any additional patient interventions. This approach will have an immediate impact in prostate and lung cancer that currently utilize fiducials or spacers in their treatment. Such bioactive fiducials should be small, radio-opaque and able to deliver radiosensitizer over a time period relevant to radiation therapy. The radio-opacity of the markers is essential to the IGRT process and enables the fiducials to be identified in the treatment planning process. The small size of the fiducials would ensure *in situ* placement using minimally invasive methods and localized release of drug which would produce preferential sensitization of the tumor with respect to surrounding normal tissue. Radio-opacity suggests use of a high-Z material and gold is used in most fiducials available commercially. XRT treatment protocols suggest drug release time constants in the range of 2–6 weeks. Knowledge of the marker locations, in relation to the tumor and normal structure, allows for the distribution of the radiosensitizer in the vicinity of the markers which in turn enables XRT treatment planning to be optimized on the basis of the biologically effective dose.

In a recent drug-loaded fiducial modeling study, we demonstrated that, by deliberate placement of drug-coated fiducials at high-risk areas of the tumor, the biologically effective radiation dose can be enhanced *in situ*, thereby increasing the chances for local tumor control during Biologically enhanced *In-Situ* IGRT (BIS-IGRT) (Cormack *et al* 2010). The present work reports experimental results that evaluate the feasibility of constructing drug-loaded biocompatible polymer-coated gold fiducials that are capable of releasing radio-sensitizer over a period of 4 weeks or more for BIS-IGRT.

This project demonstrates a novel approach to improve the properties of gold fiducial markers currently used in IGRT. To the best of our knowledge this is the first reported work on the concept of localized drug delivery using polymeric coatings on fiducial surfaces typically used for IGRT. Earlier work has demonstrated the use of chitosan in the form of nanoparticles or gels for drug release (Kofuji *et al* 2000). Unlike these papers, our work here describes the use of chitosan thin films as a biodegradable matrix on a gold fiducial typically used in IGRT from which drug loaded NPs are released. This approach facilitates the ability to modulate

drug release through a dual release mechanism. The drug release kinetics is controlled by both the rate of chitosan and nanoparticle degradation. Earlier work (Harris *et al* 2002, Ortiz *et al* 2007) has examined drug-loaded polymer implants placed intratumorally for chemotherapy or as adjuvants for thermal ablation. There the release profiles are very short and quite different from the longer times required for IGRT. The present work examines for the first time two approaches to drug- and nanoparticle-loaded coatings on gold fiducials and examines the parameters that are necessary for clinical use of coated bioactive fiducials in IGRT.

2. Materials and methods

We have studied two approaches to nanoporous coatings on fiducials.

2.1. Free drug release from fiducial coating: Dox in PMMA

As a representative free drug and nanoporous coating system, we studied Dox as the drug and poly(methyl methacrylate) (PMMA) as the nanoporous coating material. A schematic illustrating this design platform is shown in figure 1(a). PMMA is a FDA approved biocompatible and non-biodegradable polymer used extensively in orthopedic tissue engineering both as a scaffold material and as a drug-eluting matrix (FDA 2002, Jaeblo 2010, Neut *et al* 2003, Quinn *et al* 2001). Additionally, PMMA is one of the few polymers that bind strongly to gold surfaces without leaching or detachment when immersed in the water or buffer solution. The thickness of polymer coating that is desired for the drug elution platform can be precisely controlled by polymer composition, concentration and method of application on the gold surface. Dox is a drug routinely used in cancer therapy and the strong fluorescent property exhibited by this drug makes it possible to monitor its release profile through fluorescence spectroscopy (Gultepe *et al* 2010).

2.1.1. Fabrication on gold films. Gold flat films ($1 \times 1 \text{ cm}^2$) were initially selected as the substrate since they provide a large surface area and a two-dimensional surface that is easy to fabricate. A glass cover slip measuring $1 \times 1 \text{ cm}^2$ was coated with 100 nm gold film using a sputter coater. Dox, in powder form, was mixed directly in PMMA to form a well-dispersed mixture. A representative digital camera image in figure 2(a) shows the gold surface with a thin layer of polymer coating. On the surface of these coatings, dark orange specks of Dox clusters are also visible. The desired concentration of polymer/drug mixture was deposited on the gold film to form a uniform thin film coating on the surface. The polymer was then cured, as per manufacturer's instruction, by introducing the sample in $170 \text{ }^\circ\text{C}$ oven for 30 min. Samples were then allowed to cool to room temperature and introduced in the release medium to study drug elution. Two different amounts of Dox, $4 \text{ }\mu\text{g}$ and $8 \text{ }\mu\text{g}$ were dissolved in $20 \text{ }\mu\text{L}$ of PMMA and applied as a coating on the gold film such that drug concentration on the gold films was 4 and $8 \text{ }\mu\text{g cm}^{-2}$. Another set of experiments were carried out to study the effect of additional polymer coatings on top of the drug/polymer layer. A thin layer of PMMA, approximately $20 \text{ }\mu\text{l}$, was deposited on top of the initial PMMA/Dox coating on the gold flat film surface for both the 4 and $8 \text{ }\mu\text{g cm}^{-2}$ coatings.

2.1.2. Fabrication on gold fiducials. Cylindrical gold fiducials measuring $5 \text{ mm length} \times 1.5 \text{ mm diameter}$ were obtained from Best Medical Inc., Springfield, Virginia. The fabrication of drug-loaded polymer coatings on gold fiducials was challenging due to its design and shape. Initial attempts to directly coat with PMMA/Dox mixture using the solution-based dipping method did not result in uniform coatings throughout the fiducials due to its shape and resulted

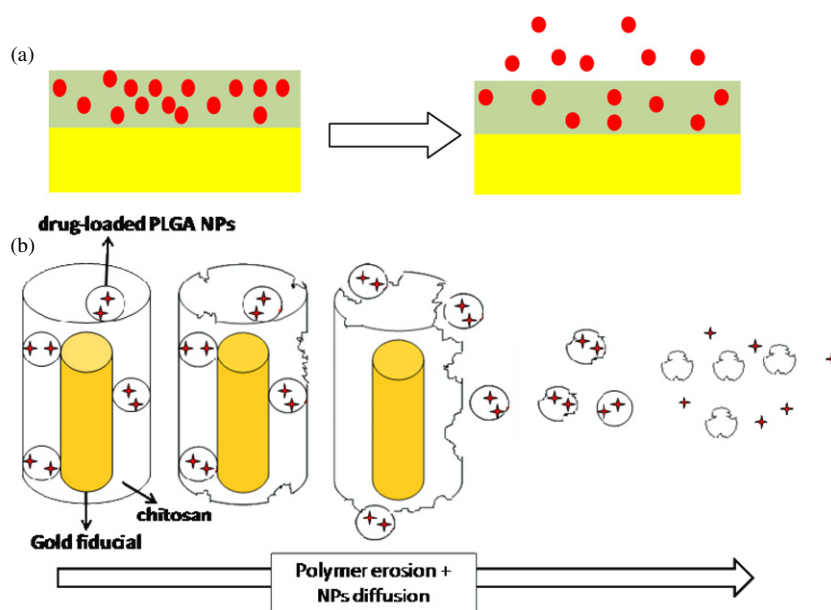


Figure 1. Schematic representation of drug release from gold fiducials. (a) Free Dox from PMMA coatings. (b) Release of drug-loaded PLGA nanoparticles from chitosan coating of fiducials. As the chitosan degradation proceeds, drug-loaded NPs are released in the medium. The drug is released from NPs when PLGA is degraded.

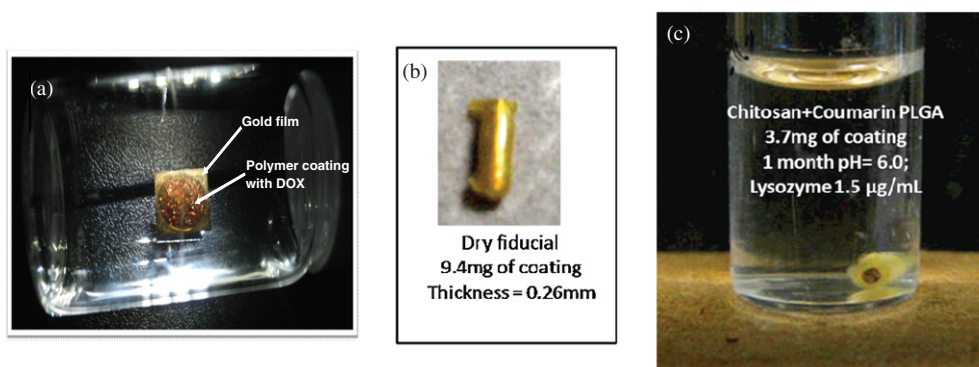


Figure 2. (a) Gold flat films with PMMA coating loaded with Doxorubicin, (b) dry and (c) wet state of gold fiducial coated with chitosan film containing Coumarin-6-loaded PLGA NPs. Orange specks of Doxorubicin embedded in the PMMA matrix on the gold film are seen in (a) and a green-yellow halo from Coumarin-6 is clearly seen from around the gold fiducial in (c).

in the polymer settling on the one side of the fiducials. To avoid this, first a layer of PDMS was deposited on the fiducial surface using a custom-built Teflon mold. Since PDMS does not stick to Teflon, PDMS-coated gold fiducials were detached from the mold. The PMMA/DOX mixture, as prepared above, was applied on top of this PDMS-coated gold fiducial. In these experiments, $2 \mu\text{g}$ of Dox was dispersed in $20 \mu\text{L}$ PMMA and coated on each fiducial such that the maximum loading of Dox was $2 \mu\text{g}$ per fiducial or $7.35 \mu\text{g cm}^{-2}$ per fiducial. In the present experiment, these loadings were chosen only because the highly sensitive fluorescence set-up (see below) saturates for more than $2 \mu\text{g}$ concentrations of fluorophore. Much higher drug loading (see section 3) is feasible for each fiducial.

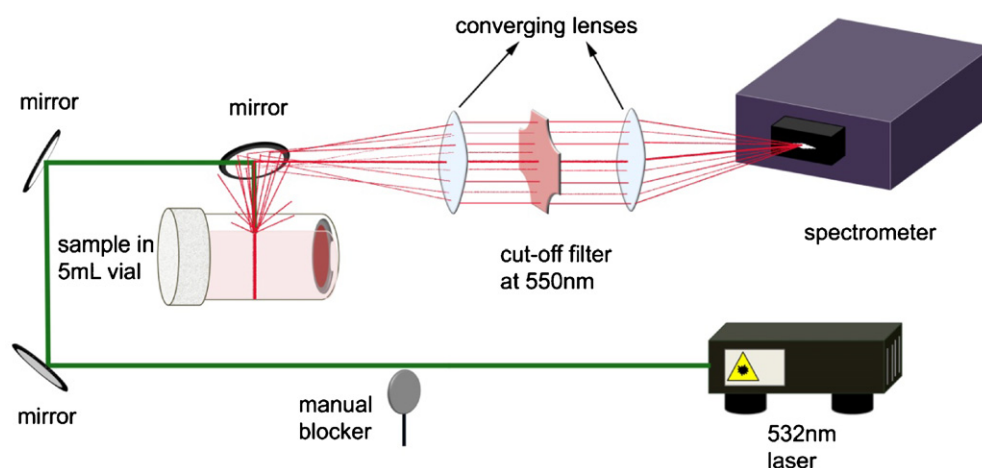


Figure 3. Experimental set-up for *in situ* fluorescence measurements (adapted from Gultepe *et al* (2010)).

2.1.3. Release profile measurement of Dox using fluorescence spectroscopy. It is important to note that these fluorescence measurements were carried out using the *in situ* spectrofluorometer set-up (figure 3, adapted from Gultepe *et al* (2010)). The design of the set-up is such that as the drug releases from the fiducials, it diffuses into the surrounding buffer medium and the fluorescence is measured from this medium. Initially, the buffer should have no drug and therefore should have no detectable fluorescence signal. As the experiment proceeds, the drug diffuses from the fiducial and fluorescence intensity in the buffer medium increases corresponding to the concentration of the drug released. The advantage of using this kind of set-up to measure release of free drug from a localized drug delivery system is the ability to collect a large number of readings without disturbing the release process. This design is critical for understanding the release kinetics since it allows the collection of fast and frequent data over time (Gultepe *et al* 2010).

The release of Dox from PMMA was performed in 1% phosphate buffered saline (PBS) at room temperature. The experimental protocol followed for this experiment is published elsewhere (Gultepe *et al* 2010). Both gold flat films and fiducials coated with Dox/PMMA were placed in glass scintillation vials with 5 mL buffer solution. The fluorescent signal, which is directly proportional to the amount of Dox in the solution, was measured directly in the release medium. A plot of fluorescence intensity of drug against different concentrations of the drug was recorded as a standard curve. When the sample for drug release was introduced in the buffer, the fluorescence signal was compared to the value in the standard curve to determine the amount of drug released from the platform. A laser beam with $\lambda_{\text{ex}} = 532 \text{ nm}$ was used to illuminate the vial at predetermined time intervals. The fluorescent emission from the vials was detected by a spectrometer (MS257 Oriel, CT). The vials were kept on a rocker in between measurements to allow for a constant mixing of the solution.

2.2. Drug-loaded nanoparticle release from the fiducial surface: Coumarin-6-loaded PLGA nanoparticles embedded in chitosan coating

In the second approach, the drug was first encapsulated inside a biodegradable polymer to form nanoparticle (NPs). These drug-loaded NPs were then mixed in a hydrogel matrix and coated on the gold fiducial. Figure 1(b) illustrates the mechanism of this nanoporous platform. As the hydrogel matrix degrades, it releases the NPs into the buffer and subsequently the free

drug is released from within these NPs into the buffer medium. This two-step method allows for a more controlled and sustained drug release over a period of time.

This approach provides two advantages: (1) the NPs can incorporate hydrophobic drugs which are not easily loaded into the matrix and (2) local delivery of drug-loaded NPs may prolong or extend drug release and exposure of tumor to the drug. Poly(D,L-lactic-co-glycolic acid) (PLGA) NPs were loaded with Coumarin-6 (m.w. 350.43 g mol⁻¹), a fluorescent model for a hydrophobic drug (e.g. Taxol). Drug-loaded NPs were embedded in chitosan gel which was applied as fiducial coating. Chitosan, a cationic bio-polymer or hydrogel, has been widely studied for biomedical application especially due to its biodegradability and biocompatibility. A notable advantage of chitosan is its film-forming capability through the solution casting technique. Many studies on drug loading, release and permeation have been performed through chitosan films (Perugini *et al* 2003, Tan *et al* 2009, Ta *et al* 2008). PLGA is another biodegradable polymer that has been widely used as nano/microparticles for drug encapsulation (Astete and Sabliov 2006, Avgoustakis 2004).

2.2.1. Preparation of Coumarin-6-loaded PLGA NPs. Three milligrams of Coumarin-6 and 0.1 g of PLGA were mixed with 4 mL dichloromethane and then combined with a mixture of 0.2 g polyvinyl alcohol (PVA) in 20 mL deionized (DI) water. This mixture was left to stir for 6 h to facilitate evaporation of chloromethane. The mixture was also covered with foil to prevent exposure to light. Once the dichloromethane evaporated, the solution was centrifuged at 4000 rpm for 10 min to remove large particles. The supernatant was then transferred to micro centrifuge tubes and centrifuged again for 15 min at 10 000 rpm to obtain particles of the desired size. The supernatant solution was discarded from each tube and the particles were transferred into one tube with 1.5 mL DI water. The size of the particles was analyzed using the Brookhaven Instruments Particle Size Analyzer 90 Plus. If there were too many large particles (>1 μm), the solution was centrifuged at 4000 rpm for another 15 min to remove these large particles. This procedure was repeated until the desired sized NPs were obtained. The particles were centrifuged at 10 000 rpm for 15 min, the water was removed and the NPs were weighed. The particles were finally suspended in 100 μL DI water and sonicated to obtain uniform dispersion.

2.2.2. Coating of Chitosan with drug-loaded NPs on gold fiducials. Gold fiducials were coated in layers with Chitosan film containing PLGA NPs. First, a suspension of NPs in Chitosan was prepared by mixing 200 μL of Chitosan gel (3% by mass and 2% by volume acetic acid) to the NP solution. The suspension was vortexed until a homogeneous suspension was obtained. The fiducial was immersed in a suspension of PLGA NPs in Chitosan gel and dried under a nitrogen stream. The procedure was repeated several times to obtain the desired thickness. The coated fiducial was further dried under vacuum for 3 h. In order to control the solubility and biodegradation of Chitosan films (Ren *et al* 2005, Verheul *et al* 2009), the coated fiducial was acetylated through the following steps: (a) immersion in the aqueous solution of sodium hydroxide (4M), (b) washing with methanol, (c) immersion in the methanol solution of acetic anhydride (4M) and (d) washing with methanol. The fiducials were finally dried in air and were ready for drug elution experiments. The mass of coating was measured by weighing the fiducials before and after coating and was found to be 3.1 ± 1.4 mg. The thickness of NPs loaded hydrogel coating as shown in figure 2(b) was 0.26 mm. Figure 2(c) is a representative image of a chitosan film containing NPs coated on gold fiducial in the wet state inside the release buffer solution. The presence of Coumarin-6 (from within the NPs) on gold fiducial

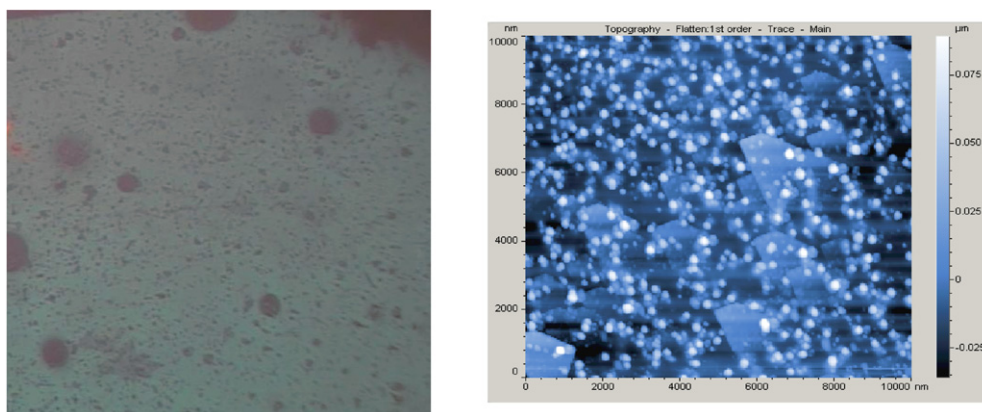


Figure 4. Images of Dox in PMMA coatings on gold films before release studies. (Left) Optical image of a $450\ \mu\text{m} \times 300\ \mu\text{m}$ area of the coating showing Dox-rich regions (red) in the PMMA matrix (white). (b) Atomic force microscopy (AFM) topography of a $1\ \mu\text{m} \times 1\ \mu\text{m}$ area showing nanoscale surface morphology. The colormap indicates the variation of surface height with position. The AFM image does not distinguish between different chemical species, but shows that the films are nanoporous and rough allowing for diffusion and elution of small molecules.

is indicated by the green-yellow halo around the fiducial. The total drug loading on each fiducial, as measured by fluorescence spectroscopy, was $17\ \mu\text{g}$ of Coumarin-6.

2.2.3. Release profile measurement of Coumarin-6 using fluorescence spectroscopy. Measurements of the release of drug-loaded NPs and of drug from NPs were performed at $37\ ^\circ\text{C}$ and $\text{pH} = 6.0$ in 1% PBS buffer in the presence of lysozyme. Lysozyme ($1.5\ \mu\text{g mL}^{-1}$) was added to the buffer in a concentration similar to that in human serum (Muzzarelli 1997). This enzyme has been recognized as the main agent responsible for depolymerizing *N*-acetylated chitosan *in vivo*. Depolymerization of chitosan occurs by the hydrolysis of glycosidic bonds present in the polysaccharide. Degradation of chitosan releases the drug-loaded PLGA NPs into the buffer medium and then the free drug is released into buffer medium when PLGA starts to degrade.

Coated fiducials were incubated with 2 mL of hepes buffer saline ($\text{pH} = 6.0$) at $37\ ^\circ\text{C}$. At particular time intervals, the buffer solution was completely withdrawn and replaced with fresh buffer. The fluorescence of the collected buffer was measured and the Coumarin-6 present (from within the NPs) in solution was quantified against the standard curve.

To determine the release of Coumarin-6 from PLGA NPs, at pre-determined time intervals, NP suspension in buffer was centrifuged at 10 000 rpm ($g = 7200$) for 15 min. The supernatant was collected and placed in cuvettes for fluorescence measurements. NPs were re-dispersed in 2 mL of fresh buffer solution. The concentration of Coumarin-6 present in solution was quantified against the standard curve.

3. Results and discussion

3.1. Dox in PMMA coatings on gold films and fiducials

The first step in this project was to understand the surface morphology of the polymer films deposited on the gold surfaces. The optical microscope image in figure 4(a) clearly shows the

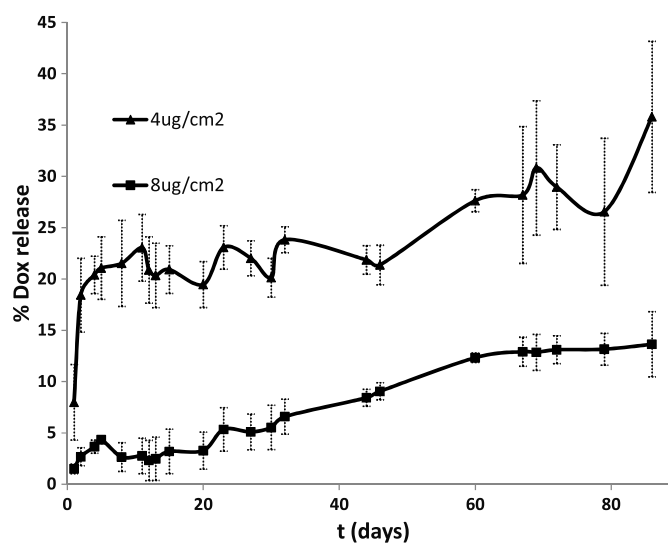


Figure 5. Release profile of Dox from PMMA coatings on gold films.

large clusters of drug molecules embedded in the polymer matrix. This is consistent with the digital camera image, as shown in figure 2(a), which shows large pockets of orange specks arising from clusters of Dox. Atomic force microscopy (AFM) was also used since it allows understanding of the nanoporous nature of the polymer coatings deposited on gold films. A representative scanned area of the gold flat film sample prior to being introduced in the release medium is shown in figure 4. The area scanned in the AFM mode was $1 \times 1 \mu\text{m}$ and a large number of particles in the size range of 100–300 nm were seen. This is different from the digital camera image, shown in figure 2(a), which shows large orange specks which correspond to Dox clusters. The AFM image indicates that in addition to big clusters of drug molecules that can be seen by the naked eye and digital camera, there is a whole range of nanometer scale morphology evenly distributed throughout the polymer film surface. The image shown here is only a representative area and these nanoscale features were seen throughout the entire surface. The voids indicate nanoscale porosity that enables drug diffusion and release. It should be pointed out that AFM does not distinguish directly between different chemical species such as Dox and PMMA but is useful for understanding film morphology to visualize features that can affect the drug release profile.

3.1.1. Release of free Dox from PMMA on the gold film. The release of Dox from the gold film was monitored by fluorescence spectroscopy and the measured release profiles are shown in figure 5. When introduced in the release medium, in both the samples, there was an initial release of Dox within the first few hours and followed by a sustained release over the course of the next 3 months. This type of release, known as the burst release, is typical for the polymer-drug delivery system (Huang and Brazel 2001). This initial burst release is from the drug molecules that are localized in the top layer of the polymer coating. After this initial burst release, drug molecules from the inner core of the polymer film diffused out resulting in a slow and sustained release of the drug. In the case of the sample with $4 \mu\text{g cm}^{-2}$, approximately 20% of Dox was released during the burst release and another 15% at the end of 3 months when the experiments were terminated. For the $8 \mu\text{g cm}^{-2}$ sample, approximately 2.5% Dox

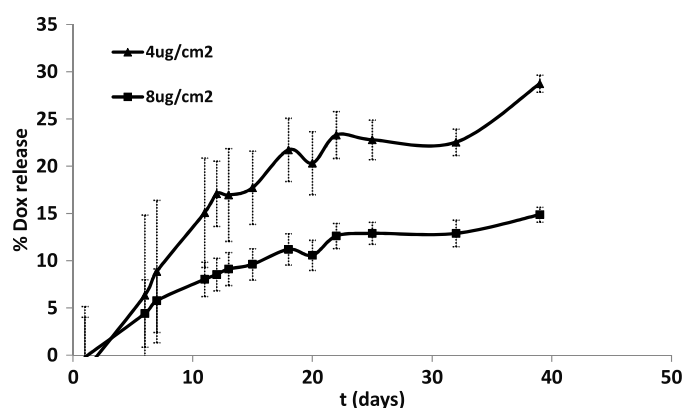


Figure 6. Release profile of Dox from PMMA coatings on gold films with suppressed burst release achieved using an extra dead layer.

was released initially and at the termination of experiment a total of about 10% was released from the gold flat films.

The difference in the release profile for the two different drug concentrations is the miscibility of Dox within the PMMA matrix. Dox is a hydrophilic drug and PMMA has degrees of hydrophobicity associated with it. Due to the issue of miscibility at this concentration, different loading and release behaviors are noticed for Dox in PMMA. In case of higher concentration, $8 \mu\text{g cm}^{-2}$ sample, more drug molecules cluster together and are pushed toward the interior of the PMMA matrix. This resulted in a much longer release time for all of the loaded drug molecules to diffuse out of the PMMA matrix. However, in the case of $4 \mu\text{g cm}^{-2}$ sample, Dox clusters are localized more toward the top layer of the PMMA matrix resulting in the release of higher concentration of drug during burst release. Therefore, the release of Dox from within PMMA matrix is dependent on the concentration of Dox, the ratio of PMMA/Dox and the thickness of PMMA/Dox coating on the gold surface. This platform allows for clever manipulation of all these properties and hence can be tailored to the desired release profile. In this case, it was a slow and sustained release for over 3 months.

Experiments were also carried out to control the initial burst release of drug from nanoporous coatings. The coating of an additional layer of PMMA was able to control the rapid diffusion of high concentration of Dox from the surface. In the case of the $4 \mu\text{g cm}^{-2}$ Dox sample, with the additional layer of PMMA, the burst release of Dox after 5 days decreased from $\sim 20\%$ to less than 5% (figure 6). Therefore, by carefully selecting the initial concentration of Dox in PMMA and thickness of additional coating of PMMA on the surface, it is possible to control the burst release of Dox from the gold film surface. There are some advantages of having this type of release system: an initial burst release within the first few days followed by a long and slow release over the course of 3 months. The initial burst will facilitate rapid establishment of a steady-state radio-sensitizer distribution around the fiducial, depending also on the behavior of the drug within tissue (Cormack *et al* 2010), prior to commencement of radiation therapy (e.g. prostate brachytherapy). However, the ability to control the initial burst release to only have one type of free drug release behavior might be useful for some applications where radiation treatment is not expected to commence until after 2 weeks from the time of fiducial implantation (e.g. prostate external beam therapy). It should be noted that these experiments were carried out to demonstrate the feasibility of

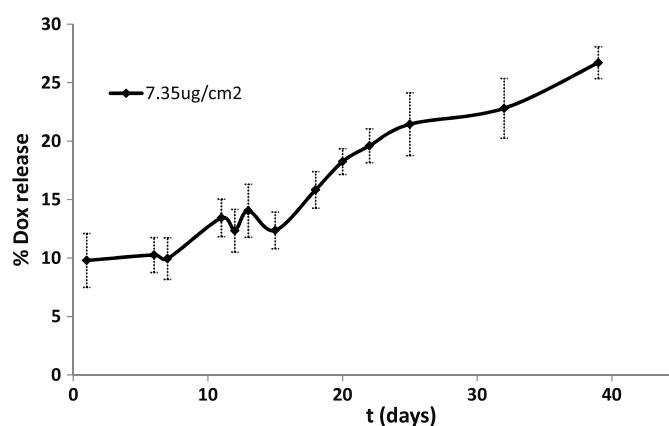


Figure 7. Release profile of Dox from PMMA coatings on gold fiducials.

both drug loading and its subsequent release from nanoporous coatings on gold fiducials. Drug loading can be further increased if necessary by increasing the drug concentration in the polymer film and/or by increasing the thickness of polymer coatings to achieve the desired drug concentration that is clinically relevant.

3.1.2. Release of Dox from PMMA on gold fiducials. These gold fiducials were introduced in the release buffer and release of free Dox was measured. As expected, an initial burst release was observed, during which $\sim 10\%$ of Dox diffused into the release medium in 1 day (figure 7). During the subsequent 40 days, there is a slow and sustained release of Dox, $\sim 25\%$ of loaded drug. Results from this experiment demonstrated the feasibility of Dox release from gold fiducials. As with the gold film, drug loading can be increased by either increasing the drug concentration in polymer or by increasing the thickness of polymer coating on the fiducial.

3.2. Release of drug-loaded nanoparticles in chitosan coatings on gold fiducials

In the second approach, as illustrated in figure 1(b), drug-loaded polymer NPs first diffuse out of the degradable matrix coated on the gold fiducial. The coated gold fiducials were placed in the HEPES buffer and at the time of fluorescence measurement, the buffer solution was completely withdrawn and replaced with fresh buffer. This method allows for collecting fluorescence data of Coumarin-6 from within the NPs and not from free Coumarin-6 from degraded PLGA NPs. The time frame for data collection, 1 day, is sufficient only to release NPs from chitosan and not degradation of PLGA NPs to release Coumarin-6. The release profile of NPs from chitosan film (figure 8) showed a continuous release of NPs from the coating during 40 days with $\sim 63\%$ of NPs being released in 20 days. After that the release became slower and additional 37% of release was observed in the next 20 days. This release rate is important for guaranteeing the presence of the drug close to the fiducial during the treatment period, which is normally 40 days.

The *in situ* fluorescence measurement used in the Dox/PMMA approach was not practical in this case to measure fluorescence from Coumarin-6. When exposed to lysozyme and buffer solution, the chitosan matrix starts to degrade and releases PLGA NPs into the surrounding medium along with flakes of chitosan. These pieces and NPs, due to their size, settle down

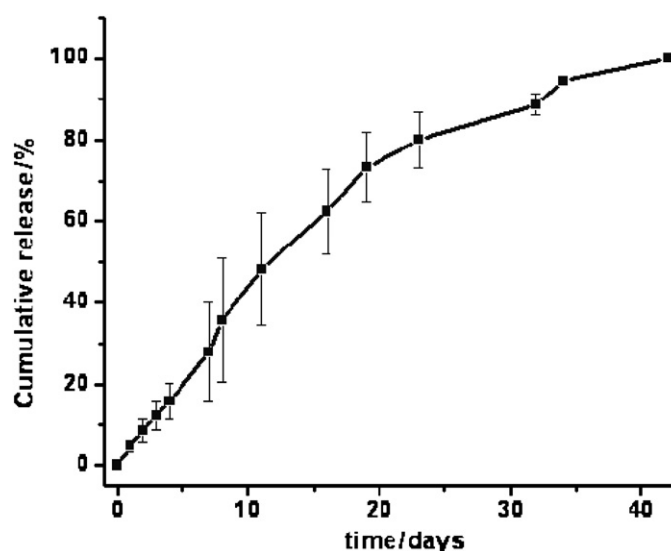


Figure 8. *In vitro* release of drug-loaded PLGA NPs from coated fiducials incubated with buffer solution (pH = 6.0) in the presence of lysozyme ($1.5 \mu\text{g mL}^{-1}$).

in the vial and therefore fluorescence from Coumarin-6 could not be detected. Therefore, in these experiments, at the necessary time points, aliquots of solution were taken from the buffer and fluorescence measured using a spectrofluorometer.

In addition to the release of NPs from the coating, it is important to characterize the release of drug from within the NPs when they are free in the solution (figure 9). NPs showed slow release in the first 2 days, when only 5% of drug was released in the solution. During the following 10 days, the release was faster and $\sim 70\%$ of drug was released in the solution. The additional 25% of drug was released in 15 days. The continuous release of drug from the NPs during 30 days indicated that NPs will be able to release the drug while they diffuse through the tumor. Furthermore, the slow drug release may avoid the fast clearance of drugs from the tumor as has been reported for the application of free drugs. In this way, the drug distribution in the tumor will depend on the NPs diffusion through the tissue. It is important to note that all these parameters may be changed as a function of the number of coating layers, concentration of NPs in the gel or concentration of drug entrapped within the NPs.

Substrate effects. The chemical composition of the substrate fiducial material does not have a direct effect on the elution. Thus, we expect that similar results should hold for other implant substrates like titanium. The drug elution is first controlled by the rate of degradation of the chitosan polymer coatings to release the NPs and subsequently the rate of degradation of NPs controls the release of drug. However, the binding of chitosan film to the fiducial surface will depend on the substrate chemical composition.

Dosage and fiducial drug loading. Harris *et al* (2002) present the time-dependent levels of Dox over several days and the data demonstrate that the Dox concentration remains high (an average of $2 \mu\text{g g}^{-1}$ of prostate) over 24 h, following which it falls to near 0. From these data, one may calculate the total cumulative micrograms of Dox in prostate. For example, a 50 g prostate will receive locally 100 μg Dox over 24 h.

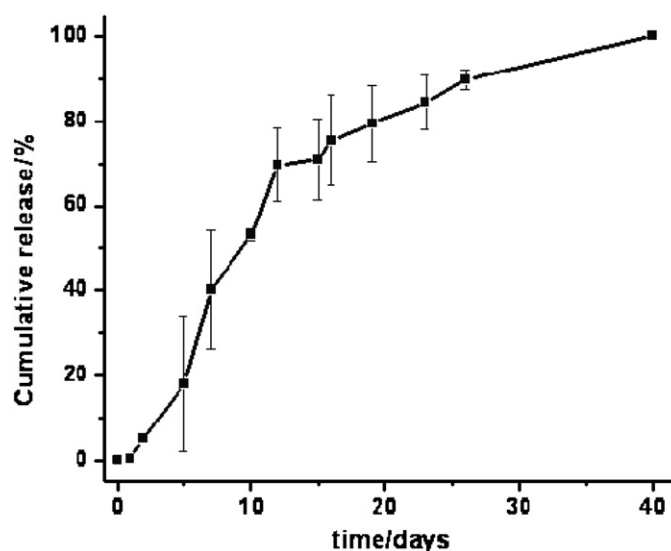


Figure 9. *In vitro* release of coumarin-6 from PLGA NPs incubated with buffer solution (pH = 6.0) in the presence of lysozyme ($1.5 \mu\text{g mL}^{-1}$).

For BIS-IGRT upto 6 fiducials are used and we would need $16 \mu\text{g}$ of Dox per fiducial (= total $100 \mu\text{g}$ of Dox). Although in the present work examining the releases kinetics we loaded only $2 \mu\text{g}$ of Dox or $17 \mu\text{g}$ of Coumarin-6 per fiducial due to the very high sensitivity of the *in situ* fluorescence set-up, much higher drug loading densities are feasible since loading of 1.6 mg Dox in 4 mm^3 polymer volumes has been reported (Ortiz *et al* 2007). Since implant coatings (of typical thickness $< 1 \text{ mm}$) are comparable in volume $\sim 5\text{--}10 \text{ mm}^3$, therapeutically relevant drug loadings of 1 mg of Dox per fiducial are definitely achievable. Radiosensitization is expected to require lower drug concentrations than chemotherapy alone and hence the present work suggests that the drug loading requirements for fiducials can be achieved.

4. Conclusion

In this work, we have taken the currently used radio-opaque gold fiducials and modified them to demonstrate the fabrication of two different kinds of drug-loaded polymer coatings for localized drug delivery within the tumor. A chemotherapeutic drug, Dox, was loaded into PMMA coatings on gold flat films and fiducials, and this platform showed continuous and diffusion limited release of the drug over 2 months that is dependent on the film thickness and drug concentration. For gold fiducials coated with chitosan film containing Coumarin-6-loaded PLGA NPs, the continuous release of NPs from coated fiducials and of drug from within PLGA NPs was observed over time periods that are consistent with IGRT treatment schedules. By careful planning of the position of the gold markers within the tumor, concomitant with manipulation of the surface of these gold fiducials with polymer thin films, radiosensitizers can be selectively delivered in therapeutically significant amounts from these fiducials during IGRT. The two nanoporous platform designed in this work demonstrates the feasibility of enhancing IGRT treatment through localized delivery of radiosensitizers (BIS-IGRT). Thus, these polymer-coated gold fiducial markers show promise as dual-functioning implants,

providing both guidance for radiation therapy and *in situ* delivery of drugs. Future work is planned to study the release kinetics *in vivo*, and the combined effect of radiosensitization and IGRT, in animal models.

Acknowledgments

We thank the anonymous referees for numerous suggestions regarding the paper. This work was supported by the Nanomedicine Science and Technology Program (NSF-DGE-0504331), by a Kayes Scholars Award, by Dana Farber-Brigham and Women's Cancer Center and Electronics Materials Research Institute at Northeastern University.

References

- Astete C E and Sabliov C M 2006 Synthesis and characterization of PLGA nanoparticles *J. Biomater. Sci. Polym. Ed.* **17** 247–89
- Avgoustakis K 2004 Pegylated poly(lactide) and poly(lactide-co-glycolide) nanoparticles: preparation, properties and possible applications in drug delivery *Curr. Drug Deliv.* **1** 321–33
- Cormack R A, Sridhar S, Suh W W, D'Amico A V and Makrigiorgos G M 2010 Biological *in situ* dose painting for image-guided radiation therapy using drug-loaded implantable devices *Int. J. Radiat. Oncol. Biol. Phys.* **76** 615–23
- Doiron A, Yapp D T, Olivares M, Zhu J X and Lehnert S 1999 Tumor radiosensitization by sustained intratumoral release of bromodeoxyuridine *Cancer Res.* **59** 3677–81
- FDA 2002 Available at <http://www.fda.gov/MedicalDevices/DeviceRegulationandGuidance/GuidanceDocuments/ucm072795.htm>
- Friedland J L, Freeman D E, Masterson-McGary M E and Spellberg D M 2009 Stereotactic body radiotherapy: an emerging treatment approach for localized prostate cancer *Technol. Cancer Res. Treat.* **8** 387–92
- Garcia-Garcia H M, Vaina S, Tsuchida K and Serruys PW 2006 Drug-eluting stents *Arch. Cardiol. Mex.* **76** 297–319
- Gultepe E *et al* 2010 Sustained drug release from non-eroding nanoporous templates *Small* **6** 213–6
- Huang X and Brazel C S 2001 On the importance and mechanisms of burst release in matrix-controlled drug delivery systems *J. Controlled Release* **73** 121–36
- Jaebblon T 2010 Polymethylmethacrylate: properties and contemporary uses in orthopaedics *J. Am. Acad. Orthop. Surg.* **18** 297–305
- Harris K A, Harry E and Small E J 2002 Liposomal doxorubicin for the treatment of hormone-refractory prostate cancer *Clin. Prostate Cancer* **1** 37–41
- Kofuji K, Ito T, Murata Y and Kawashima S 2000 The controlled release of a drug from biodegradable chitosan gel beads *Chem. Pharm. Bull.* **48** 579–81
- Kumar P 2003 A new paradigm for the treatment of high-risk prostate cancer: radiosensitization with docetaxel *Rev. Urol.* **5** (Suppl. 3) S71–7
- Li Y, Owusu A and Lehnert S 2004 Treatment of intracranial rat glioma model with implant of radiosensitizer and biomodulator drug combined with external beam radiotherapy *Int. J. Radiat. Oncol. Biol. Phys.* **58** 519–27
- Muzzarelli R A A 1997 Human enzymatic activities related to the therapeutic administration of chitin derivatives *Cell. Mol. Life Sci.* **53** 131–40
- Neut D, van de Belt H, van Horn J R, van der Mei H C and Busscher H J 2003 Residual gentamicin-release from antibiotic-loaded polymethylmethacrylate beads after 5 years of implantation *Biomaterials* **24** 1829–31
- Ortiz R, Au J L-S, Lu Z, Gan Y and Wientjes M G 2007 Biodegradable intraprostatic doxorubicin implants *AAPS J.* **9** E241–50
- Perugini P, Genta I, Conti B, Modena T and Pavanetto F 2003 Periodontal delivery of ipriflavone: new chitosan/PLGA film delivery system for a lipophilic drug *Int. J. Pharm.* **252** 1–9
- Quinn R H, Mankin H J, Springfield D S and Gebhardt M C 2001 Management of infected bulk allografts with antibiotic-impregnated polymethylmethacrylate spacers *Orthopedics* **24** 971–5
- Ren D, Yi H, Wang W and Ma X 2005 The enzymatic degradation and swelling properties of chitosan matrices with different degrees of *N*-acetylation *Carbohydr. Res.* **340** 2403–10
- Ta H T, Dass C R and Dunstan D E 2008 Injectable chitosan hydrogels for localised cancer therapy *J. Controlled Release* **126** 205–16
- Tan M L, Choong P F and Dass C R 2009 Review: doxorubicin delivery systems based on chitosan for cancer therapy *J. Pharm. Pharmacol.* **61** 131–42

- Verheul R J, Amidi M, van Steenberg M J, van Riet E, Jiskoot W and Hennink W E 2009 Influence of the degree of acetylation on the enzymatic degradation and in vitro biological properties of trimethylated chitosans *Biomaterials* **30** 3129–35
- Wurm R E *et al* 2006 Image guided respiratory gated hypofractionated stereotactic body radiation therapy (H-SBRT) for liver and lung tumors: initial experience *Acta Oncol.* **45** 881–9
- Xie Y, Djajaputra D, King C R, Hossain S, Ma L and Xing L 2008 Intrafractional motion of the prostate during hypofractionated radiotherapy *Int. J. Radiat. Oncol. Biol. Phys.* **72** 236–46 [PMCID: 2725181](#)